International Journal of Advanced Science and Technology
Vol. 29, No.02, (2020), pp. 996-1006

# An Efficient Enhancement Method for Finger Vein Images Using Double Histogram Equalization

Khamis A.Zidan[1] Shereen S.Jumaa[2]
[1]*AL-Iraqia university,Baghdad,Iraq.*
[2], *College ofInformation Engineering, Al-Nahrain University,Baghdad , Iraq.*

***Abstract:***

*With the advent of latest technological breakthroughs, it has become quite an easy feat to hack the commonly used biometrics such as face, voice and fingerprint etc. This has led to the exploration of new vistas in this domain.One of the most secure biometrics of today is finger vein- but this high degree of security comes with its own challenges, the most prominent one being that the vein pattern is extremely difficult to extract because finger vein images are always low in quality, gravely hampering the feature extraction and classification stages. Sophisticated algorithms need to be designed for this purpose. The aim of this paper is to present a computationally light-weight yet highly efficient procedure that can be used to extract the vascular pattern from a person's finger illuminated by infrared radiation.Experiment results demonstrate that the proposed method is not only efficiently lightweight with regard to computational time but also achieves state –of-the art results by clearly bringing out the enhanced vascular pattern beneath finger skin*

***Keywords****: Efficient, stage*

## Introduction

Information security of this age and day is being dominated by the use of biometric technology- the technique of identifying a person based on biological traits such as physical or behavioral characteristics(1).Physical biometrics include iris, hand geometry, face, fingerprint etc.and behavioral biometrics include gait, voice, signature, keystroke pattern etc. Most of these traits are prone to hack attempts (2,3) and so this had led to the development of more secure biometrics such as vein patterns within finger (4)hand(5)and palm(6). These are nearly impossible to attain without the users' consent and hence harder to forge. In this paper we will present a new method of enhancement of finger vein data. Vein data can only be acquired from a living body so cannot be obtained from a deceased body(7).Vascular structure lies beneath the skin, and so is impossible to observe(8)without special equipment such as infrared radiation and camera etc. Acquisition process is contactless, so hygiene is ensured and user convenience is warranted(9).Majority of the state of art methods of finger vein recognition suffer from drawbacks associated with feature extraction due to images of low quality and poor vein visibility. Low quality images may be attributed to bad quality of infrared radiation, poor lightening conditions, and scattering of light in tissues surrounding the vein structure that is desired to be captured(6). Complications may also arise in case of obese finger, low environment temperature or improperly designed capturing equipment(7). Another parameter that greatly hampers the process is that a vast majority of such algorithms depend on parameters that cannot be set as a defined standard over different databases. A change in finger alignment in training and testing data may also gravely effect results for segmentation based as well as statistical methods.

**Database:**
It is a fact universally agreed (8,9)that the toughest finger vein database to preprocess is SDUMLA-HMT database as shown in Fig.1. Following are the reasons for this non-ideality:

- Its quality of images is not good(10).
- Finger area is very small compared to overall image size(10).
- Images vary in rotation, translation and shift(11).
- An uncontrolled image capturing method was deployed (8).

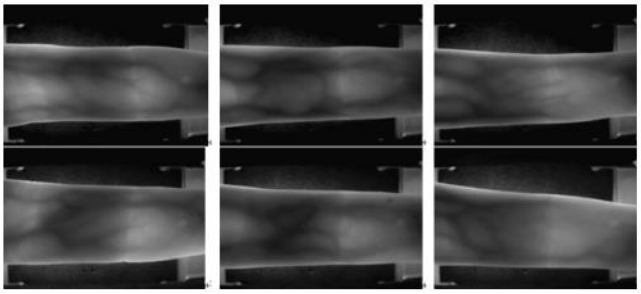

**Figure 1. SDUMLA-HMT database- sample data.**
This is the reason that we chose this database for the validation of our algorithm. A total of 106 individuals took part in its compilation. Images captured are in .bmp format. Right and left hands both were used. For each hand, data of index, middle and ring fingers was captured (12)and for each finger, 6 samples were obtained as shown in Table 1. The device used for this purpose was designed by Joint Lab for Intelligent Computing and Intelligent Systems of Wuhan University.

**Table 1 . SDUMLA database at a glance.**

| Parameter | Information |
|---|---|
| **Total persons** | 106 |
| **Hands per person** | 2 |
| **Fingers per hand** | 3 |
| **Images per finger** | 6 |
| **Image resolution** | 320 × 240 |
| **Total size of database** | 0.85 b |

**Methodology**
Methodology employed consists of only a few selected basic enhancement operators that are simple to implement and computationally light- yet when combined together in sequence as shown in Fig.2, they yield a highly accurate enhanced version of the finger vein image.

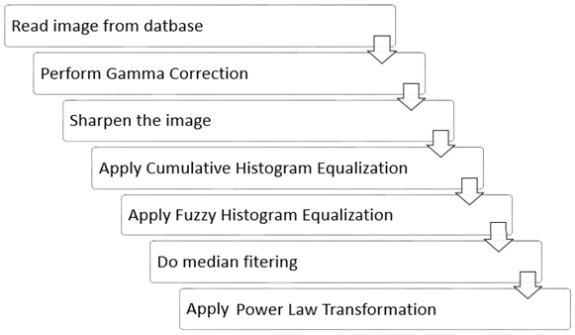


**Figure 2. Presented methodology.**
The steps of presented method as following:
**Detection of finger**

Database images are captured by throwing near-infrared radiation on finger. The veins, owing to the flow of deoxygenated hemoglobin, absorb this radiation, thus appearing darker than the surrounding tissue(13) as shown in Fig.3.

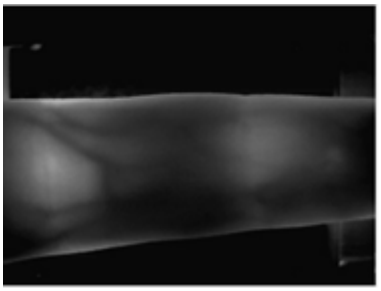

**Figure 3 . Database image of person 56, left hand, middle finger.**

First step is to detect and crop the finger region from this image. Mask filter was used for this localization following the procedure attempted by(14).Texture was extracted after normalization of finger region. Mask is generated on the basis that finger region is lighter in contrast as compared to rest of the image region. The approach of (14) was used to localize the finger region by using a mask filter. Finger region was normalized and texture was extracted from it. It is based on the principle that finger region is brighter than background region since infrared light passes through it. The mask used to segment out the finger region of a database image, resembles the images as shown in Fig. 4 :

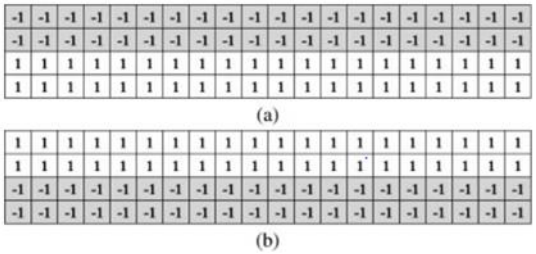


**Figure 4. Masks for localizing the finer regions of the captured images. (a) Mask for detecting the upper region of the finger. (b) Mask for detecting the lower region of the finger.**

Boundary of the finger is detected by computing the masking value in y dimension for each value along the x dimension. Point of maximization of this masking value is actually the boundary of the finger in y direction(15).After that the database image is cropped by retaining the portion of only those rows which are fully white on the corresponding mask as shown in Fig.5.

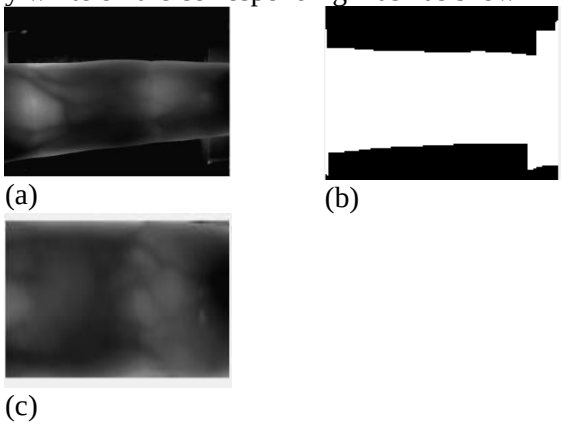

**Figure 5. (a) Database image (b) Mask obtained .(c) Cropped finger .**

**Gamma correction**

Since the cropped finger is quite dark, so next step is the enhancement of its brightness using Gamma correction(16,17).It works by enhancing the dynamic range of pixel intensities by non-linearly manipulating the pixels. It is achieved by minimizing the homogeneity of co- occurrence matrix. This enables the underlying details to be brought to surface and made more prominent(18,19). It boosts image quality to a great deal by steering the average brightness of an image in the direction desired.

For the case of proposed algorithm, it was observed that if gamma parameter is kept to be 2, it gives most optimum results as shown in Fig. 6.

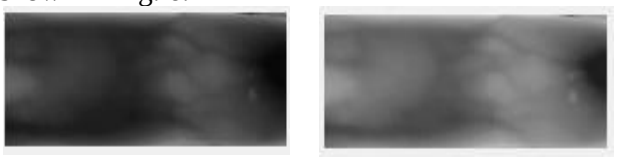

(a) (b)

**Figure 6.(a)Before Gamma correction (b) After Gamma correction**

**Vein sharpening**

Although the gamma corrected version of the image has better brightness than the original image, but there is still room for improvement where the prominence of veins is concerned. To further bring out the vascular structure, the algorithm of unsharp masking is used to sharpen the image. This is performed so as to improve the contrast between various ranges of pixel intensities(20). It brings those suppressed visual details to foreground that would otherwise have been missed by human eye.Image sharpening does not actually create any detail, it only enhances the hidden details and texture of an image. The process starts by creating an "unsharp: or blurred version of an image. This version is then subtracted from the original to detect the presence of edges. Contrast is then selectively increased along the detected edges yielding a much sharper version of the image(21,22).

The unsharp mask we deployed for our experiments is created by using a Gaussian filter for spatially filtering the gamma enhanced version of finger vein image. This filter is basically obtained by convolution operation of the image with kernel mask as shown in Fig. 7. Standard deviation of Gaussian low pass filter is the parameter than controls the area around the edges that is enhanced during the sharpening procedure. Its value was kept to be 4 in implemented methodology. A larger value influences a larger portion of the surrounding area and vice versa. Sharpening strength was also kept to be 4 during experiments.

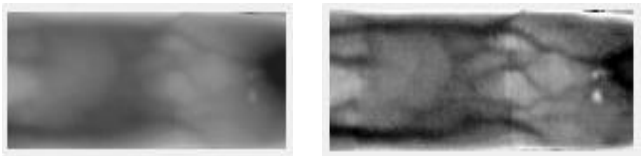

(a) (b)

**Figure 7. (a) Image Before Sharpening, (b) Image After Sharpening**.

**Double Histogram Equalization**

Next step was to perform histogram equalization to adjust the intensity distribution of pixel values. We opted for a double histogram equalization that contains the strengths of Fuzzy Histogram Equalization with Cumulative Histogram Equalization. The basic purpose of using histogram equalization is to spread out the pixel intensity histogram more evenly to increase the dynamic range of pixels which in turn increases contrast.

Cumulative histogram equalization was performed first. It was then followed by Fuzzy histogram equalization.

**Cumulative histogram equalization**

Cumulative histogram equalization of an image is performed as in equ.(1) by the following steps(23):

1. Obtain image histogram.
2. Obtain histogram of cumulative distribution function.

3. Use histogram equalization formula to find a new corresponding value for each gray value of original image.

If:

total number of pixels= N

total number of possible intensity levels= L

then(25),

$$S_k = \frac{L}{N} * C_R(k) - 1 \qquad (1)$$

Here k represents an original intensity value and is in an integer that varies from 0 to L-1, and Sk is the mapped intensity value

1. Replace each gray value of the original image with its corresponding newly computed value from the above step.

Vein sharpening gives image as shown in Fig.8(a) and its corresponding histogram is shown in Fig.8(b).

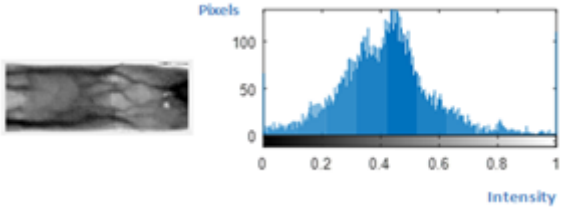


(a) (b)

**Figure 8.Before Histogram equalization (a) Image (b) Histogram**.

After Cumulative histogram equalization, we get the image as shown in Figure 9(a). Its histogram as shown in Fig. 9(b) is nearly flat as compared to Fig. 8(b).

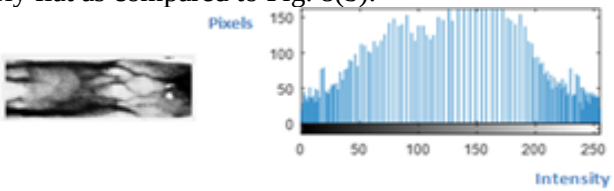


(a) (b)

**Figure 9. After Cumulative Histogram equalization (a) Image (b) Histogram.**

A closer look at the flattened histogram of Fig. 9(b) shows that although the histogram is more evenly distributed than that of Fig. 8(b) but at the horizontal edges of the graph, there is an overcrowding of pixel intensities. To counter this effect, fuzzy histogram equalization was performed next.

**Fuzzy histogram equalization**

Brightness preserving dynamic fuzzy histogram equalization(24) manipulates the image histogram such that no remapping of peaks takes place. It uniformly redistributes the histogram values only in valley-areas between two consecutive peaks. It consists of the following steps (25):

1. Fuzzy Histogram Computation
2. Histogram Partitioning
3. Dynamic Histogram Equalization of Partitions
4. Normalization of image brightness if needed

Fuzzy statistics is able to handle the inexactness of gray values in a much better way compared to classical crisp histograms thus producing a smooth histogram as shown in Fig.10. This makes it highly suitable for equalizing the above histogram .

A fuzzy histogram is a sequence of real numbers

h(i), i ∈ {0, 1, …., L-1} where h(i) is the frequency of occurrence of gray levels that are "around i ". Each gray value I(x,y) is considered a fuzzy number I~(x,y) as shown in equ.(2). Fuzzy histogram is then computed as:

$h(i) \leftarrow h(i) + \sum_x \sum_y \mu_{I(x,y)i}$ , $k \in [a, b]$ (2)

Here in equ.(3) $\mu_{I(x,y)i}$ is the triangular fuzzy membership function given by:

$$\mu_{I(x,y)i} = \max[0, 1 - \frac{|I(x,y)-i|}{4}] \quad (3)$$

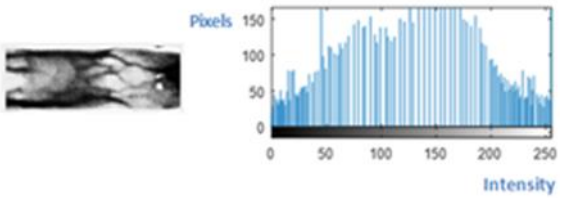


(a) (b)

**Figure10.After Fuzzy Histogram equalization (a) Image (b) Histogram.**

**Median filtering**

The image processed by double histogram equalization is then made to pass through a median filter so as to remove impulsive noise and salt- and- pepper noise through this nonlinear process. For each pixel, a window is used to select neighboring pixels. Then median intensity value is computed for the pixels within this window and that value is assigned to the pixel on which the operation was being performed. This process is repeated for all pixels of the image (26).It preserves the edge-information while smoothly removing noise. Strength of median filter depends upon window size (27). For the experiments of this research, we used window size of 3x3 as shown in Fig .11.

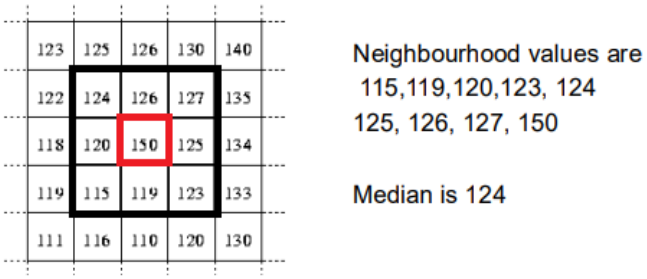


**Figure 11. Median filtering using 3x3 window size (18).**

It soothes out the irregularities within texture as shown in the image in Fig.12 :

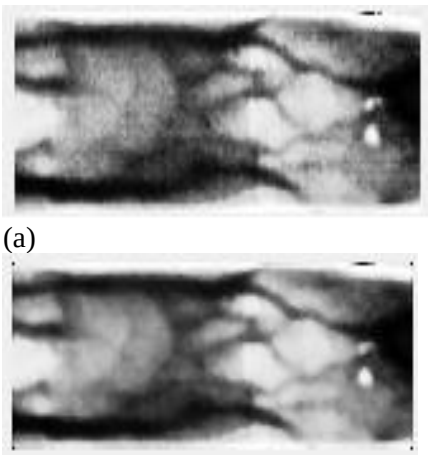

(a)

(b)

**Figure 12. (a) Before median filtering (b) After median filtering**

**Power law**

As a final step, power law transformation was applied to the image to enhance contrast and improve visibility. Power law transform is represented by the equ.(4),(28)

$$S = CR^{\gamma} \qquad (4)$$

Here C and $\gamma$ are positive constants. $\gamma$ may be a positive value less than or greater than 1. For C=1, if $\gamma < 1$ then the input image is transformed into an image with a wider range of pixel intensities (thus making the image brighter) and if $\gamma > 1$ then image is transformed by mapping it into a narrower range of pixel intensities (thus making it appear darker(29).

For the purpose of our experiments, we kept C=1 and $\gamma$=0.3. In this technique, power law curves with fractional values of $\gamma$ mapped the median- filtered finger vein image (which had a darker range) to a transformed image (which had a broader range of pixels). Final enhanced image corresponding to Fig.12 is shown in the Fig.13.

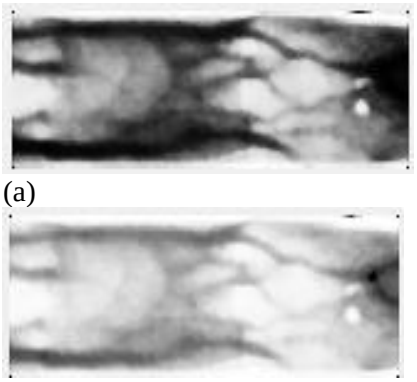

(a)

(b)

**Figure 13. (a) Before Power law transform, (b) After Power law.**

**Experimental results:**

The visual results of proposed method can be summarized in Table 2 on a few sample images from the SDUMLA HMT database.

To evaluate the proposed method, two evaluation metrics were used: Peak Signal to Noise Ratio (PSNR) and Structural Similarity Index (SSIM).

PSNR is a classic metric that is commonly used to measure the quality of a restored image. Higher the value of PSNR, better is the quality of an image. It's the ratio of maximum intensity to the mean square error between the image and its reference counterpart. It is given by the equ.5 (30):

$$PSNR = 10log_{10}\frac{MaxI^2}{Mean\ square\ error} \qquad (5)$$

For the purpose of experimentation in this research, we computed PSNR at each stage with reference taken as the initially cropped finger from database image. For the four sample images shown in Table 2, PSNR results are compiled in the Table 3.

Second evaluation measure considered was SSIM. For the evaluation of image quality, SSIM is widely regarded as the most suitable measure (30). It is a much more reliable measure than PSNR and MSE. Computation of SSIM depends not only on the image itself but also on a reference image(31). For the purpose of results evaluation of our work, we compared image after each stage with the image of the original finger that was directly cropped from the database image. SSIM basically compares thecontrast and structural details between two images. It is an evaluation metric that is universally used to assess the quality of bio-medical images. It is computed by the following formula in equ.(6,7,8,9,10,11):

$$SSIM = \frac{2(\mu_x+\mu_y)(2\delta_{xy})}{(\mu_x^2+\mu_y^2)(\delta_x^2+\delta_y^2)} (6)$$

Where

$$\mu_x = \frac{1}{N}\sum_{i=1}^{N} x_i (7)$$

$$\mu_y = \frac{1}{N}\sum_{i=1}^{N} y_i (8)$$

$$\delta_x = \sqrt{\frac{1}{N-1}\sum_{i=1}^{N}(x_i-\mu_x)^2} \quad (9)$$

$$\delta_y = \sqrt{\frac{1}{N-1}\sum_{i=1}^{N}(y_i-\mu_y)^2} (10)$$

$$\delta_{xy} = \frac{1}{N-1}\sum_{i=1}^{N}(x_i-\mu_x)(y_i-\mu_y) (11)$$

| Process | Sample image # 1 | Sample image # 2 | Sample image # 3 | Sample image # 4 |
|---|---|---|---|---|
| **Database image** | 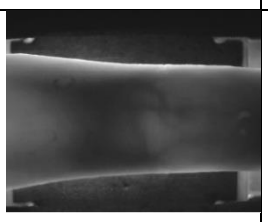 | 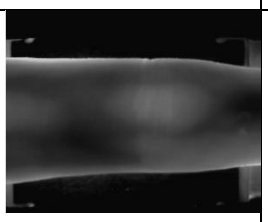 | 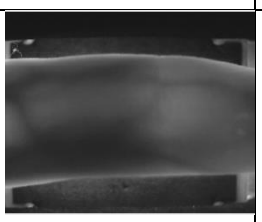 | 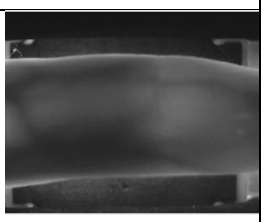 |
| **Cropped finger** |  |  |  |  |
| **Gamma correction** |  |  | 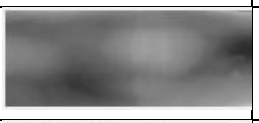 | 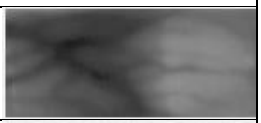 |
| **Image sharpening** | 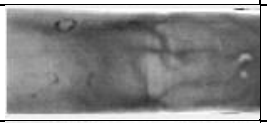 | 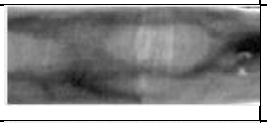 | 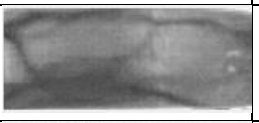 |  |
| **Cumulative Histogram Equalization** |  | 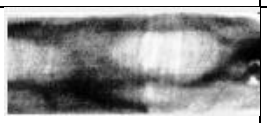 |  |  |
| **Fuzzy Histogram Equalization** |  | 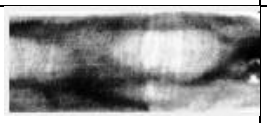 |  |  |
| **Median filtering** | 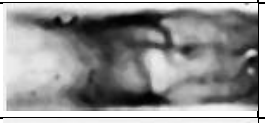 | 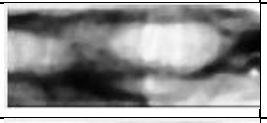 |  | 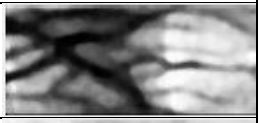 |
| **Power Law transform** | 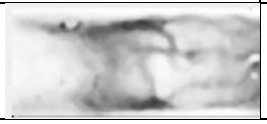 |  |  | 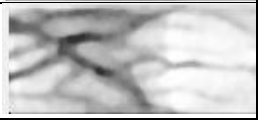 |

**Table 2 .Results of method on sample images from SDUMLA dataset.**

**Table 3. PSNR results after each step**

| Stage | Sample image #1 | Sample image #2 | Sample image #3 | Sample image #4 |
|---|---|---|---|---|
| **Gamma correction** | 52.9658 | 53.8044 | 51.0154 | 56.4074 |
| **Image sharpening** | 53.62 | 52.9123 | 51.2777 | 55.0926 |
| **Cumulative Histogram Equalization** | 4.6915 | 4.706 | 4.7042 | 4.7256 |
| **Fuzzy Histogram Equalization** | 4.7088 | 4.7218 | 4.7229 | 4.7422 |
| **Median filtering** | 4.9538 | 4.9711 | 4.9959 | 4.9524 |
| **Power Law transform** | 48.7389 | 48.5594 | 48.5717 | 48.5588 |

Its value varies between 0 and 1. SSIM of two exactly same images is 1. Lesser the similarity between two images, closer this value is to 0. For the case of our experiments, we needed to find the difference between image structure at a given stage and that at the initial stage, so we subtracted the value of SSIM from 1 so as to get the change in image structure and these values are displayed in the Table 4. This Table of SSIM values, shows the amount of change in visual structural information. Greater this value, greater is the change in image after a given operation.

**Table 4: Change in SSIM after each step.**

| Stage | Sample image #1 | Sample image #2 | Sample image #3 | Sample image #4 |
|---|---|---|---|---|
| **Gamma correction** | 0.038221 | 0.032068 | 0.064663 | 0.017573 |
| **Image sharpening** | 0.030202 | 0.038539 | 0.057303 | 0.021713 |
| **Cumulative Histogram Equalization** | 0.99891 | 0.99373 | 0.99889 | 0.99919 |
| **Fuzzy Histogram Equalization** | 0.99905 | 0.99546 | 0.99904 | 0.99926 |
| **Median filtering** | 0.99836 | 0.99515 | 0.99862 | 0.99894 |
| **Power Law transform** | 0.11147 | 0.11829 | 0.11741 | 0.11685 |

Experimental analysis showed that the presented method is not only robust in performance but also achieves state of the art results in negligible time as documented in the Table 5.

**Table 5. Average computational time per step**

| Preprocessing Stage | Average time taken (seconds) |
|---|---|
| **Finger detection** | 0.0072 |
| **Gamma correction** | 0.0011 |
| **Image sharpening** | 0.0036 |

| | |
|---|---|
| **Cumulative Histogram Equalization** | 0.0028 |
| **Fuzzy Histogram Equalization** | 0.0031 |
| **Median filtering** | 0.0066 |
| **Power Law transform** | 0.0014 |

**Conclusion and future work:**

This paper presented a new algorithm for the enhancement of finger vein images. The strongest point about this methodology is its low computational complexity which renders it a perfect choice for use in high level applications like real time finger vein recognition and verification. It consists of steps that are not only efficient but also simple to implement. SDUMLA database was used for analysis of presented methodology. Firstly, finger was detected from the database image. It was followed by gamma correction. Next, the image was sharpened using 'unsharp' masking technique. Histogram equalization was performed twice: first cumulative histogram equalization and then fuzzy histogram equalization. Cumulative histogram equalization served to flatten the overall shape of the histogram and fuzzy histogram equalization worked on the overcrowded areas between consecutive histogram peaks to make them uniform. After that, median filtering was applied to remove the remnant undesirable effects of sharpening if any. It made the texture smoother while preserving the shape of vascular skeleton. Power law was applied as the last step to enhance contrast and improve visibility. As a future extension of this work, recognition and verification might be implemented following the presented enhancement procedure. Also this technique might be tested on palm vein, dorsal hand vein and wrist vein data. This method can be further extended to measure the diameter of veins. This application could be particularly useful in the detection of diseases such as Cirrhosis(32) that affect vein thickness.

**References**

1. Syazana-Itqan K, Syafeeza AR, Saad NM, Hamid NA, Saad WM. A review of finger-vein biometrics identification approaches. .Indian J. Sci. Technol. 2016 Aug;9(32)
2. Marcel S, Nixon MS, Li SZ. Handbook of biometric anti-spoofing. New York: Springer; 2014.
3. Menotti D, Chiachia G, Pinto A, Schwartz WR, Pedrini H, Falcao AX, Rocha A. Deep representations for iris, face, and fingerprint spoofing detection. IEEE Transactions on Information Forensics and Security. 2015 Apr;10(4):864-79.
4. Kumar A, Zhou Y. Human identification using finger images. IEEE Transactions on image processing. 2012 Apr;21(4):2228-44.
5. Wen X, Zhao J, Liang X. Research on enhancing human finger vein pattern characteristics. In2010 Asia-Pacific Conference on Power Electronics and Design 2010 May 30 (pp. 97-100). IEEE.
6. Lee EC, Park KR. Image restoration of skin scattering and optical blurring for finger vein recognition. Optics and Lasers in Engineering. 2011 Jul 1;49(7):816-28.
7. Yang L, Yang G, Yin Y, Xi X. Finger vein recognition with anatomy structure analysis. IEEE Transactions on Circuits and Systems for Video Technology. 2018 Aug;28(8):1892-905.
8. Meng X, Xi X, Yang G, Yin Y. Finger vein recognition based on deformation information. Science China Information Sciences. 2018 May 1;61(5):052103.
9. Abdulsahib, G. M., & Khalaf, O. I. (2018). Comparison and Evaluation of Cloud Processing Models in Cloud-Based Networks. International Journal of Simulation--Systems, Science & Technology, 19(5).
10. Yang L, Yang G, Yin Y, Xi X. Finger vein recognition with anatomy structure analysis. IEEE Transactions on Circuits and Systems for Video Technology. 2018 Aug;28(8):1892-905.
11. Yang Y, Yang G, Wang S. Finger vein recognition based on multi-instance. International Journal of Digital Content Technology and its Applications. 2012 Jun;6(11):86-94.

12. Kim W, Song J, Park K. Multimodal Biometric Recognition Based on Convolutional Neural Network by the Fusion of Finger-Vein and Finger Shape Using Near-Infrared (NIR) Camera Sensor. Sensors. 2018 Jul;18(7):2296.
13. Akintoye KA, Rahim MS, Abdullah AH. Challenges of Finger Vein Recognition System: A Theoretical Perspective. ARPN Journal of Engineering and Applied Sciences, 2018.
14. Lee EC, Lee HC, Park KR. Finger vein recognition using minutia-based alignment and local binary pattern-based feature extraction. International Journal of Imaging Systems and Technology. 2009 Sep;19(3):179-86.
15. Park KR, Jang YK, Kang BJ. A study on touchless finger vein recognition robust to the alignment and rotation of finger. The KIPS Transactions: PartB. 2008;15(4):275-84.
16. Amiri SA, Hassanpour H. A preprocessing approach for image analysis using gamma correction. International Journal of Computer Applications. 2012 Jan;38(12):38-46.
17. Somasundaram K, Kalavathi P. Medical image contrast enhancement based on gamma correction. .Int J Knowl Manag e-learning. 2011 Jan;3(1):15-8
18. Osamah Ibrahim Khalaf, Ghaida Muttashar Abdulsahib and Muayed Sadik, 2018. A Modified Algorithm for Improving Lifetime WSN. Journal of Engineering and Applied Sciences, 13: 9277-9282
19. Hassanpour H, Samadiani N, Salehi SM. Using morphological transforms to enhance the contrast of medical images. The Egyptian Journal of Radiology and Nuclear Medicine. 2015 Jun 1;46(2):481-9.
20. Kansal S, Purwar S, Tripathi RK. Image contrast enhancement using unsharp masking and histogram equalization. Multimedia Tools and Applications. 2018 Oct 1:1-20.
21. Abdulsahib, G. M., & Khalaf, O. I. (2018). Comparison and Evaluation of Cloud Processing Models in Cloud-Based Networks. International Journal of Simulation--Systems, Science & Technology, 19(5).
22. Xiurong T. The application of adaptive unsharp mask algorithm in medical image enhancement. InProceedings of 2011 Cross Strait Quad-Regional Radio Science and Wireless Technology Conference 2011 Jul 26 (Vol. 2, pp. 1368-1370). IEEE.
23. Garg P, Jain T. A Comparative Study on Histogram Equalization and Cumulative Histogram Equalization. International Journal of New Technology and Research.;3(9).
24. Oakes WC, Zoltowski CB. Phenomenography: A Qualitative Research Method to Inform and Improve the Traditional Aerospace Engineering Discipline.
25. Sheet D, Garud H, Suveer A, Mahadevappa M, Chatterjee J. Brightness preserving dynamic fuzzy histogram equalization. IEEE Transactions on Consumer Electronics. 2010 Nov;56(4):2475-80.
26. Nagu M, Shanker NV. Image de-noising by using median filter and weiner filter. International Journal of Innovative Research in Computer and Communication Engineering. 2014 Sep;2(9):5641-9.
27. Makandar A, Halalli B. Breast cancer image enhancement using median filter and CLAHE. International Journal of Scientific & Engineering Research. 2015;6(4):462-5.
28. Janani P, Premaladha J, Ravichandran KS. Image enhancement techniques: A study. Indian Journal of Science and Technology. 2015 Sep;8(22):1-2.
29. Ramiz MA, Quazi R. HYBRID TECHNIQUE FOR IMAGE ENHANCEMENT.International Research Journal of Engineering and Technology, 2017.
30. Rajkumar S, Malathi G. A comparative analysis on image quality assessment for real time satellite images. Indian J Sci Technol. 2016 Sep;9:1-1.
31. Ece C, Mullana MM. Image quality assessment techniques pn spatial domain. IJCST. 2011 .Sep;2(3)
32. Khalaf, O. I., & Sabbar, B. M. (2019). An overview on wireless sensor networks and finding optimal location of nodes. Periodicals of Engineering and Natural Sciences, 7(3), 1096-1101.